Technical Note: Stability of tris pH buffer in artificial seawater stored in bags

Wiley H. Wolfe[1], Kenisha M. Shipley[1], Philip J. Bresnahan[2], Yuichiro Takeshita[3], Taylor Wirth[1], Todd R. Martz[1]

[1]Scripps Institution of Oceanography, University of California San Diego, La Jolla, 92093, USA
[2]Department of Earth and Ocean Sciences, University of North Carolina Wilmington, Wilmington, 28403, USA
[3]Monterey Bay Aquarium Research Institute, Moss Landing, 95093, USA

Correspondence To: Philip J. Bresnahan Jr. (bresnahanp@uncw.edu)

10 **Abstract**

11   Equimolal tris (2-amino-2-hydroxymethyl-propane-1,3-diol) buffer in artificial seawater is a well characterized
12 and commonly used standard for oceanographic pH measurements. We evaluated the stability of tris pH when stored
13 in purportedly gas impermeable bags across a variety of experimental conditions, including bag type, and storage in
14 air vs. seawater over 300 days. Bench-top spectrophotometric pH analysis revealed that the pH of tris stored in bags
15 decreased at a rate of 0.0058 ± 0.0011 yr^{-1} (mean slope $\pm$ 95% confidence interval of slope). Analyses of total dissolved
16 inorganic carbon confirmed that a combination of CO_2 infiltration and/or microbial respiration led to the observed
17 decrease in pH. Eliminating the change in pH of bagged tris remains a goal, yet the rate of pH change is lower than
18 many processes of interest and demonstrates the potential of bagged tris for sensor calibration and validation of
19 autonomous in situ pH measurements.

20 **1. Introduction**

21   Ocean pH is a key measurement used for tracking biogeochemical processes such as photosynthesis,
22 respiration, and calcification (Takeshita et al., 2016); and represents perhaps the most recognized variable associated
23 with ocean acidification (OA), the decrease in ocean pH due to the uptake of anthropogenic carbon dioxide (Doney et
24 al., 2009). OA progresses with a global average pH decline of 0.002 per year in the surface open ocean (Bates et al.,
25 2014), and the accumulated and projected near-term effects of OA have been shown to have deleterious effects on
26 many calcifying organisms (Cooley and Doney, 2009). Beyond the narrow scope of calcifiers, organismal response is
27 complex, exhibiting varied responses across processes such as reproduction, growth rate, and sensory perception.
28 Organismal responses are further complicated by their impact on ecosystem level dynamics, such as altering
29 competition and predator-prey relationships (Doney et al., 2020). Furthermore, pH effects are often exacerbated by
30 concomitant stressors, such as decreased dissolved oxygen or increased temperature. Ultimately, OA will affect
31 humans through impacts on fisheries, aquaculture, and shoreline protection (Branch et al., 2013; Doney et al., 2020).
32   The quality of pH measurement required to observe various phenomena is often broken into "climate" and
33 "weather" levels of uncertainty (Newton et al., 2015), or 0.003 and 0.02, respectively. Discrete sampling has been
34 shown to be capable of meeting the climate level of uncertainty when best practices are followed, yet many labs do
35 not consistently meet this standard (Bockmon and Dickson, 2015). Furthermore, while discrete, bench-top
36 methodologies can be the most accurate, the ocean's vast size limits the oceanographic community's ability to make
37 ship-based discrete pH measurements to decadal reoccupations of a few major sections per ocean basin (Sloyan et al.,
38 2019). The sparsity of ship-board measurements hinders our ability to assess sub-decadal processes, such as seasonal
39 cycles or bloom events, over much of the ocean (Karl, 2010), and highlights the need for autonomous, high-frequency
40 pH measurements. Technological advancements have led to more routine autonomous pH measurements over the past
41 decade, providing opportunities to fill some gaps in time and space in discrete sampling programs (e.g, Byrne, 2014;
42 Martz et al., 2015; Lai et al., 2018; Wang et al., 2019; Tilbrook et al., 2019). Globally, pH sensors now operate on
43 hundreds of autonomous platforms including moorings and profiling floats, delivering unique datasets in the form of
44 Eulerian and depth resolved Lagrangian time series (Johnson et al., 2017; Bushinsky et al., 2019; Sutton et al., 2019).

62 While sensors increase data coverage, many sensor-based pH measurements, particularly on moored systems, continue
63 to fall short of both climate and weather levels of uncertainty, as highlighted in the intercomparison tests carried out
64 by the Alliance for Coastal Technologies (ACT, 2012) and by the Wendy Schmidt Ocean Health XPRIZE (Okazaki
65 et al., 2017).

66 Independent validation is typically required for autonomous sensors to meet both weather and climate levels
67 of uncertainty. For example, autonomous underway pCO$_2$ systems (Pierrot et al., 2009), moorings (Bushinsky et al.,
68 2019), and autonomous surface vehicles (Chavez et al., 2017; Sabine et al., 2020) are able to provide climate quality
69 observations with an uncertainty of $\pm$ 2 µatm because traceable standard gases are frequently measured in situ. For pH
70 measurements on profiling floats (Johnson et al., 2016), sensor performance is validated by comparing to a deep
71 reference pH field that is calculated using empirical algorithms (Williams et al., 2016; Bittig et al., 2018; Carter et al.,
72 2018). This approach has demonstrated the ability to obtain high quality pH measurements from a network of profiling
73 floats (Johnson et al., 2017) but requires measurements in the deep ocean where pH is comparatively stable. It is
74 atypical for other pH sensors, including coastal moored sensors, to have an automated or remote validation. Therefore,
75 on such deployments, validation has largely relied on discrete samples taken alongside the sensor (Bresnahan et al.,
76 2014; McLaughlin et al., 2017; Takeshita et al., 2018), which presents unique challenges; primarily that spatiotemporal
77 discrepancy can lead to errors of > 0.1, especially in highly dynamic systems (Bresnahan et al., 2014).

78 Similar to the method in use by pCO$_2$ systems, one approach to validate in situ pH sensors is by measuring a
79 reference material or pH standard, repeatedly during a sensor deployment. The most commonly used standard for
80 oceanographic pH measurement is equimolal tris (2-amino-2-hydroxymethyl-propane-1,3-diol) buffer in artificial
81 seawater (ASW), hereafter referred to as tris or tris-ASW (DelValls and Dickson, 1998; Papadimitriou et al., 2016).
82 The pH of tris has been characterized over a range of temperature, salinity, and pressure (DelValls and Dickson, 1998;
83 Rodriguez et al., 2015; Takeshita et al., 2017; Müller et al., 2018), allowing for accurate calculation of tris pH across
84 a wide range of marine conditions. Furthermore, when stored in borosilicate bottles and under ideal conditions, these
85 buffers have been shown to be stable to better than 0.0005 over a year (Dickson, 1993; Nemzer and Dickson, 2005),
86 making tris a good candidate for in situ validation of long term deployments of autonomous pH sensors. To be utilized
87 for in situ applications, the reference solution must be stored in bags (as in, Hales et al., 2005; Seidel et al., 2008;
88 Sayles and Eck, 2009; Spaulding et al., 2014; Wang et al., 2015; Lai et al., 2018). Recently, in situ sensor validation
89 using bagged tris was demonstrated by Lai et al. (2018) during a 150-day deployment of an autonomous pH sensor,
90 where the tris standard was measured in situ every 5 days. However, the stability of tris when stored in bags has not
91 been quantified systematically using spectrophotometric bench-top pH measurement techniques recommended as best
92 practices (Dickson et al., 2007).

93 In this work we quantified the stability of tris stored in bags for 300 days. Tris from four separately prepared
94 batches was stored in two bag types either in a lab or submerged in seawater. In addition, one batch was stored in
95 borosilicate bottles in the lab as a control. Spectrophotometric pH measurements were made approximately every two
96 months on each bag of tris. Throughout the experiment, Certified Reference Materials (CRMs) for oceanic CO$_2$
97 measurements (Dickson, 2001) were used to assess the stability of the spectrophotometric pH system.

2. Methods

105

106   Two bag types were tested for storing tris (Figure 1). Bag type 1 was custom made based on a design used in

107   the "Burke-o-Lator" system (Hales et al., 2005; Bandstra et al., 2006), made from PAKDRY 7500 barrier film

108   (IMPAK P75C0919). The barrier film is made of layers of polyester and nylon with a sealant layer of metallocene

109   polyethylene. Two 23 x 48 cm (9" x 19") sheets were heat sealed on three sides, forming a pocket, and a 1.9 cm (¾")

110   diameter hole was cut into one of the pocket walls for the bulkhead fitting and bulkhead nut (McMaster-Carr

111   8674T55). The bulkhead was sealed into the wall with a silicone gasket (McMaster-Carr 9010K13), washer

112   (McMaster-Carr 95649A256), and coated with silicone sealant (McMaster-Carr 74955A53). A "push-to-connect" ball

113   valve fitting (McMaster-Carr 4379K41), was attached to the bulkhead. The modified pocket was rinsed, dried, and

114   heat sealed along the final edge to create a ~4 L bag. Bags were left to dry for at least 24 hours before filling. Bag type

115   2 was a commercially available 3 L Cali-5-Bond bag purchased from Calibrated Instruments and used without

116   modification. It is a multi-layer bag made of plastic, aluminium foil (to prevent liquid and gas permeation), a layer of

117   inert high density polyethylene (to form a non-reactive inner wall) and, a polycarbonate Stopcock Luer valve.
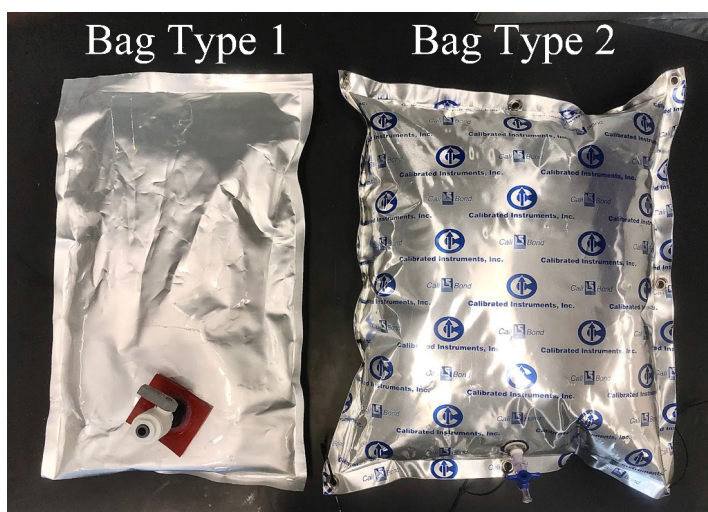
Figure 1: A picture of bag type 1 and 2 used to store tris in this study.

118   In this experiment, four batches of tris were prepared following the procedure in DelValls and Dickson

119   (1998), using off-the-shelf reagents with no additional standardization or purification (e.g. recrystallization of salts).

120   The focus of this paper is stability of bagged tris over time and does not prioritize obtaining highly accurate equimolal

121   tris (as would be necessary for characterization of thermodynamic constants, for example). The calculated pH of tris

122   in this study was 8.2652 at 20°C, based on quantity of reagents used. This is 0.0135 higher than the pH of equimolal

123   tris, 8.2517 at 20°C (DelValls and Dickson, 1998). The pH discrepancy was due to a unit error in the measurement of

124   HCl (our preparation used mol/L rather than the prescribed mol/kg-sol). This unit error resulted in a tris:trisH$^+$ of

125   1:0.97 that slightly differs from the 1:1 of truly equimolal tris. As this ratio is nearly equimolal, the term "equimolal"

130 will continue to be used throughout this study. The details of the specific reagents used to prepare the tris solution can

131 be found in Table A1.

132   Three stability tests were initiated at different times over the course of 18 months. The initiation of a given

133 test is defined as the date of preparation of the tris used in that test. A summary of the differences between these tests

134 is shown in Table 1 and described here. Each bag has a unique identifier in the format of "Batch #, Bag #, Lab or

135 Tank." If this identifier is duplicative, the bags are differentiated with letters A to D. Each bag was rinsed before

136 filling: 3 times with deionized water (DI), 5 times with ultrapure water (> 18 MΩ resistivity) and at least 3 times with

137 200 mL of tris. Tris bags were stored on a lab bench or in a 5,000 L test tank filled with ozone-sterilized, filtered

138 seawater. Bag type 2 experienced delamination of exterior layers when stored in seawater during test 2 and was not

139 used in further testing. Tris from batch 4 was also stored in borosilicate bottles following the procedure in Nemzer

140 and Dickson (2005). In addition to pH measurements, dissolved inorganic carbon (C_T) was measured on both bagged

141 and bottled tris during test 3 to see if changes in pH were due to increased CO_2. C_T samples were measured using a

142 custom-built system based on an infrared (IR) analyser (LI-COR 7000) similar to systems used by O'Sullivan and

143 Millero (1998) and Friederich et al. (2002). This IR measurement system is capable of measuring relatively low C_T

144 without requiring method adjustment and has been used to make near zero C_T measurements (Paulsen and Dickson,

145 unpublished data). C_T measurements were made on CRMs (Batch 179 & 183). The precision of the C_T measurements

146 was ± 1.4 μmol/kg (pooled standard deviation, $n_{samples}$=15, $n_{measurements}$=44).

147 **Table 1: Tris preparation and storage.**

	Bag Type	Tris Batch	Date Made	Storage Location	Rinse Procedure	C_T Measured
Test 1	1 & 2	1 & 2	13 Dec 2017	Lab & Tank	3x DI, 5x ultrapure, 3x tris	No
Test 2	1 & 2	3	13 April 2018	Lab & Tank	3x DI, 5x ultrapure, 3x tris	No
Test 3	1 & bottle	4	26 February 2019	Lab	3x DI, 5x ultrapure, ≥ 6x tris	Yes

148

149   Tris pH was measured every 55 ± 20 days (mean ± standard deviation of measurement interval) throughout

150 the experiment. The pH of tris was measured in triplicate at each time point with spectrophotometry using m-cresol

151 purple as the indicator dye using the system described in Carter et al. (2013). Absorbance measurements were made

152 in a 10-cm jacketed cell, and the temperature was measured directly adjacent to the cell outflow using a NIST-traceable

153 thermometer (± 0.1 °C, QTI DTU6028P-001-SC). Blank and sample were held for 3 minutes in the jacketed flow cell

154 prior to absorbance measurements.

155   On average, temperature was stable to within a 0.02 °C range over the course of the day; the mean temperature

156 throughout the experiment was 20.09 ± 0.23 °C (1 σ), although temperature was 0.6 °C higher than the average on

157 one measurement day. Spectrophotometric pH measurements are reported at 20 °C by adjusting the measured pH

158 value at the measured cell temperature T_C (pH_{spec,T_C}) to 20 °C ($pH_{spec,20°C}$) using the known temperature dependence

159 of tris (pH_{tris}) as follows:

$$pH_{spec,20°C} = pH_{spec,T_C} - (pH_{tris,T_C} - pH_{tris,20°C}) \tag{1}$$

$pH_{tris,Tc}$ and $pH_{tris,20°C}$ are the theoretical pH of tris (at the measured temperature and 20 °C respectively) and were calculated using Eq. (18) in DelValls and Dickson (1998). This adjustment assumes that any potential difference in $\partial pH/\partial T$ between that corresponding to equimolal tris and that corresponding to our 1:0.97 tris:trisH$^+$ ratio has a negligible effect over the small temperature range observed.

To account for pH-dependent errors from impurities in unpurified mCP, a pH-dependent correction factor was determined based on the protocol outlined in Takeshita et al. (in reiew). Briefly, pH of seawater was measured subsequently using impure dye (pH$_{impure}$; from Aldrich, lot MKBH6858V) and purified dye (pH$_{pure}$; from Robert Byrne's Lab, University of South Florida (Liu et al., 2011)) over a range of pH between 7.4 to 8.2 at approximately 0.2 intervals. Varying ratios of tris:trisH$^+$ were used to obtain different solution pH, and to buffer any changes in pH during the experiment, which negates the need for dye perturbation corrections in this characterization. Triplicate measurements were made at each pH. A second order pH-dependent error was observed as previously described, following the equation (R^2 = 0.975, RMSE = 0.000434):

$$pH_{pure} = -0.0047777 \times pH_{impure}^2 + 1.0668875 \times pH_{impure} - 0.2359740 \tag{2}$$

All subsequent pH$_{spec}$ measurements in this study were conducted with impure dye and are reported with this dye impurity correction (Eq. 2) applied. The correction adjusted the reported pH by 0.0093 ± 0.0002 (mean ± standard deviation, n = 126). No dye perturbation correction was used (a correction for a change in pH caused by the addition of the dye). As the high buffering capacity of tris, in combination with a dye adjusted to a pH similar to that of tris, results in a negligible change in measured pH.

Measurements of tris batches 1 and 2 made in the first 150 days have been removed from the data set due to procedural changes made to the spectrophotometric pH system to correct for problems with temperature equilibration. Outliers were removed from the spectrophotometric pH measurements if the absorbance at 760 nm was above 0.005 or below –0.002 (indicative of a measurement problem, such as a bubble or lamp drift), resulting in the removal of 2 out of 163 measurements. Additionally, outliers were removed from the data set if they were greater than three standard deviations from the mean of a measurement triplicate, where standard deviation is calculated as using all sets of triplicates (1 standard deviation = 0.0004, n = 55), resulting in the removal of 2 of 161 remaining measurements. The remaining 159 measurements were used for the analysis presented here. An analysis of variation, or ANOVA, was used to detect the dependence of the results on tris batch, bag/bottle type and storage location. Analysis was performed using MATLAB R2020a and the standard function "anovan()." Throughout the experiment, CRMs (procured from A. Dickson, Scripps Institution of Oceanography) for seawater C_T and total alkalinity were measured regularly to verify instrument performance (Dickson, 2001). A time-series of CRM measurements over the duration of the work described here showed no systematic drift. (Fig. A1 in Appendix A). To assess if the change in pH was driven by the addition of CO$_2$, the final pH and available C_T measurements were compared with a model described here. The theoretical change in tris-artificial seawater (ASW) pH due to an increase in C_T is straightforward to calculate, since both tris and CO$_2$ acid-base equilibria are well-characterized in seawater and ASW media. The pH is calculated for tris-ASW + C_T using an equilibrium model following the approach described in Chapter 2 of Dickson et al. (2007) for the case of known alkalinity and C_T. In the case of ASW, the seawater equilibrium constants for CO$_2$

are appropriate because minor ions present in seawater and not ASW do not appreciably affect the CO_2 equilibrium constants (particularly when the goal is to compute relative changes in pH) as the ionic background of ASW is closely matched to that of seawater at salinity = 35. In our model, minor acid-base species important to seawater alkalinity but not present in ASW (borate, phosphate, silicate, fluoride) are set to zero. The definition of total alkalinity is modified to include the tris acid-base system following the definition of acid-base donor/acceptor criteria given by Dickson (1981): tris is assigned as a level-1 proton acceptor and tris-H^+ is at the zero level. Thus, in our model, $tris_{tot}$ = 0.08 molal and alkalinity = 0.04 molal and C_T is a variable. An algorithm (see Annexe 1 in Dickson et al. (2007)) is then used to find the root of the alkalinity equation in its residual form by solving for pH.

3. Results & Discussion

Figure 2 depicts $pH_{spec,20°C}$, stored in either a bag or bottle, as a function of time and is subdivided for tests 1, 2, and 3. A linear decrease was observed for all bags or bottles. A linear regression was calculated for each experimental condition and, in the cases where measurements at t = 0 were removed due to protocol changes described above, the line was extrapolated back to t = 0, shown by the dotted line. The measured or extrapolated y-intercept is reported as the initial pH in Table 2. In all tests, trendlines are extrapolated to t = 365 days to illustrate observed and

251 predicted change over the course of a year as shown by the solid line. For ease of visual comparison, the y-axis of

252 each subplot has an identical pH range of 0.017.

253

254
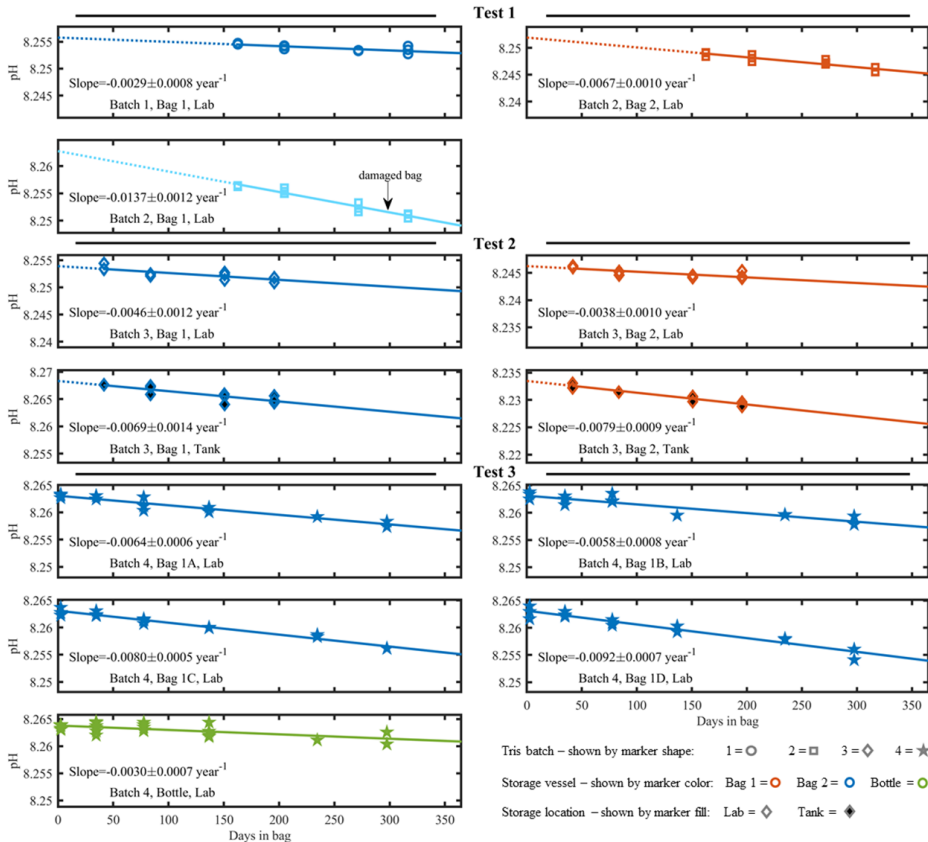
Figure 2: Individual time series of measured pH in tris buffer solutions. Bag type 1 is shown in blue (light blue for the damaged bag of type 1), 2 in orange and bottle in green. Tris batch 1 is depicted as circles, 2 as squares, 3 as diamonds and 4 as stars. Storage location in tank has a black fill and lab symbols have no fill. This marker system is also followed in Fig. A2. The solid line is a linear regression starting at the first included pH measurement and ending 365 days after the tris was bagged. The dotted line illustrates the extrapolation back to 0 days stored in bag when measurements at t = 0 do not exist. The range of the y-axis scale is fixed at 0.017 pH for all subplots.

261

Table 2: Linear regression statistics from trendlines shown in Fig. 1 and 2. The last row shows the regression statistics for tris from all batches, in either bag type, stored in the lab or test tank. Slope and intercept are shown as mean ± 95% confidence intervals. The reported intercept is the regression intercept; when initial pH measurements are available, they differ by less than 0.0003 from regression intercept. * Indicates the outlier (Batch 2, Bag 1, Lab) caused by a damaged bag. The outlier, "Batch 2, Bag 1, lab", was not used in the "All Batches, All Bags, Lab or Tank" composite. † In all batches, all bags, lab or tank, the slope was calculated with a linear fit of all (non-outlier) tris measurements. The RMSE is the mean RMSE of all (non-outlier) bag fits. ‡ The calculated tris pH was calculated at 20°C; however, this calculated pH is 0.0135 higher than equimolal tris as noted above (DelValls and Dickson, 1998).

Batch & Storage Method	Slope (mpH yr^{-1})	Intercept (Initial pH)	RMSE (mpH)	r^2	n
Batch 1, Bag 1, Lab	-2.9 ± 1.7	8.2558 ± 0.0012	0.43	0.59	12
Batch 2, Bag 1, Lab*	-13.7 ± 2.7	8.2627 ± 0.0018	0.61	0.94	11
Batch 2, Bag 2, Lab	-6.7 ± 2.2	8.2519 ± 0.0015	0.55	0.82	12
Batch 3, Bag 1, Lab	-4.6 ± 2.7	8.2539 ± 0.0010	0.62	0.62	11
Batch 3, Bag 1, Tank	-6.9 ± 3.2	8.2683 ± 0.0012	0.73	0.73	11
Batch 3, Bag 2, Lab	-3.8 ± 2.1	8.2462 ± 0.0008	0.54	0.61	12
Batch 3, Bag 2, Tank	-7.9 ± 2.1	8.2335 ± 0.0008	0.44	0.92	9
Batch 4, Bag 1A, Lab	-6.4 ± 1.3	8.2630 ± 0.0005	0.64	0.90	14
Batch 4, Bag 1B, Lab	-5.8 ± 1.8	8.2631 ± 0.0008	0.91	0.79	15
Batch 4, Bag 1C, Lab	-8.0 ± 1.0	8.2631 ± 0.0004	0.49	0.96	15
Batch 4, Bag 1D, Lab	-9.2 ± 1.6	8.2631 ± 0.0007	0.80	0.92	15
Batch 4, Bottle, Lab	-3.0 ± 1.4	8.2638 ± 0.0005	0.81	0.44	25
All Batches, All Bags, Lab or Tank†	-5.8 ± 1.1	–	0.72	0.66	126
Calculated tris pH‡	–	8.2652	–	–	–

Only bags from test 3, using tris batch 4 and bag type 1, have direct initial pH measurements and replicate bags. Initial pH measurements of these 4 bags were 8.2630 ± 0.0007 (mean ± standard deviation, n = 12). Importantly, the very low standard deviation suggests that a single initial pH measurement is representative of all replicate bags filled with a single tris batch, if the preparation procedure used in test 3 is followed. This inter-bag consistency is beneficial because it reduces the number of initial pH measurements required when filling multiple bags. There is also strong agreement in initial pH measurements between bagged and bottled tris in test 3, with the initial pH of bottled tris 0.0007 higher than bagged tris (8.26327 ± 0.0004, n = 6). The differences in filling procedure or impurities between bags and bottles in test 3 appear to have little effect on the initial pH. The mean initial pH of tris batch 4 is 0.002 (n = 5) lower than calculated pH$_{tris,20°C}$ (Fig. A2). This difference between the mean initial pH of tris batch 4 and calculated pH$_{tris,20°C}$ is similar in direction and magnitude to those reported in other studies: DeGrandpre et al. (2014) reported –0.0012 ±0.0025 and Müller and Rehder (2018) reported -0.002 to -0.008 (measured pH minus pH$_{tris,T_C}$). With standard laboratory equipment and off-the-shelf reagents, an uncertainty of 0.006 is expected in prepared tris (Paulsen and Dickson, 2020). Measurements were also made on Dickson standard tris (batch T35) using the same instrument and the pH was 0.0019 higher than the calculated pH$_{tris,20°C}$ (n = 2). In tests 1 and 2, the initial pH was extrapolated from a linear regression. The extrapolated initial pH values are more variable and lower (on average) than those directly

291 measured (Fig. A2). These differences may be a result of the extrapolation or different experimental variables such as

292 the increased rinsing of bags, or the single bag type and storage location used in test 3.
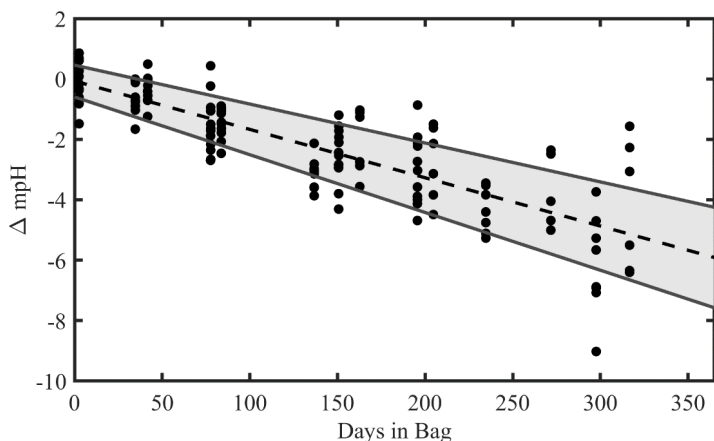
293

294 **Figure 3: Combined time series of measured pH in tris buffer tris buffer solutions. The dots represent every**
295 **measurement made on a (non-damaged) bag of tris. The dotted line is the "All Bags, All Batches, Lab or Tank"**
296 **regression. The grey shaded region is the observational 95% confidence interval (CI). The CI is intended to**
297 **estimate the future pH of a tris bag (with known initial pH and an unmeasured bag specific rate of change).**
298 **The upper and lower bounds are -0.0042 and -0.0076 pH per year, respectively.**

299   Figure 3 depicts a composite of all test results as the change from the initial pH of tris

300 $\left(\Delta pH = pH_{spec,20°C}^{t=day} - pH_{spec,20°C}^{t=0}\right)$ as a function of time elapsed since bagging. A linear regression on all pH

301 measurements, excluding the outlier of "Batch 2, Bag 1, Lab", of tris stored in bag types 1 or 2, has a slope of –0.0058

302 ± 0.0011 yr^{-1} (mean ± 95% C.I.). The upper and lower bounds of ΔpH at t = 365 days, -0.0042 and -0.0076, are

303 important to consider when utilizing this bagged storage method of tris. These bounds provide the broadest expected

304 range in pH change over a year of storage, and include both the intercept and slope confidence intervals. The outlier

305 (Batch 2, Bag 1, Lab) was excluded due to noticeable damage to the bag (see Fig. A3 in Appendix A), which is

306 believed to have caused its pH to decrease at more than two times the average rate of the other bags. The damage

307 appears to be a break in the metallic bag layer, potentially caused by creasing or pinching of the bag when handling.

308 This observation highlights the importance of maintaining bag integrity, particularly during use in the field. A

309 successful two-week field deployment has been conducted using the tris bags described here and a modified SeapHOx

310 in a shallow, coral reef flat (Bresnahan et al. 2021). This two-week deployment was significantly shorter than the year

311 of storage described here and further field testing in longer deployments in varied environments are required before

312 widespread use of this technology. For the longer time frame depicted in Figure 3, the only comparable example found

313 in the literature is the work of Lai et al. (2018). In this work, Lai et al. (2018) used bagged tris for sensor calibration,

314 with in situ tris measurements made over 150 days. Lai et al. (2018) did not report a change in the pH of bagged tris

332 over the deployment; however, the reported precision of the SAMI-pH in situ instrument (± 0.003) would not resolve

333 the expected change shown in our Figure 3. Therefore, the results of Lai et al. (2018) are not inconsistent with our

334 study.

335   A significant increase in C_T was observed for all types of bags and bottles in Experiment 3 (Figure 4). A high

336 correlation between solution pH and C_T was observed, with a slope of –0.0029 ± 0.0006 pH per 100 µmol kg^{-1} (n =

337 14, r^2 = 0.70), suggesting that the change in tris pH and C_T was primarily driven by an increase in CO_2. The observed

338 slope agrees closely with a theoretical model prediction of a linear decrease in pH of –0.0024 per 100 µmol kg^{-1} of

339 C_T added (over the range of C_T observed). There are two possible sources of the increasing C_T: gas exchange of CO_2

340 with the environment and microbial respiration within the storage vessel. Gas exchange should not be a significant

341 source of CO_2 for tris stored in a borosilicate bottle, as this is the standard equipment used to store seawater CO_2 and

342 tris buffers and is known to minimize gas exchange (Dickson et al. 2007). Therefore, it is likely that respiration was

343 the primary driver for the increase in C_T for tris stored in bottles. On average, pH decrease of tris stored in bags was

344 larger than that in the standard bottle (Figure 2), indicating either an additional source of CO_2 from gas exchange, or

345 larger amounts of respiration. Distinguishing between these two theorized sources would require measurements of

346 additional parameters such as dissolved organic carbon.

347
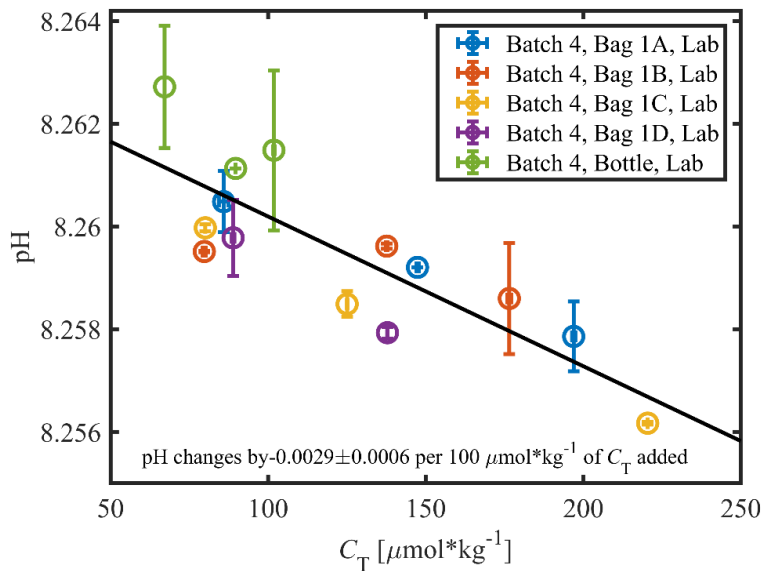
Figure 4: pH plotted against C_T shows a linear relationship between the two parameters in tris buffer with a slope of –
0.0029 pH for every 100 µmol kg^{-1} of C_T added. The measurements shown are from three sampling occurrences between
130–300 days stored on bags and bottles used in Test 3. Only two measurements are shown for "Batch 4, Bag 1D, Lab"
because it ran empty before C_T were made.

Deleted: drift

Deleted: drift

Deleted: The linear decrease was calculated using an ad hoc acid–base equilibrium model of seawater including tris in addition to the CO_2 and other minor acid–base systems.

Deleted: has been designed to

Deleted: drift

359 The pH stability of tris could be improved by reducing either likely source of C_T: gas exchange or microbial

360 respiration. For bags, CO_2 may diffuse through the fittings, gasket, or bag walls, particularly if damaged. The relatively

361 small breaks in the aluminium foil layer caused "Batch 2, Bag 1, Lab" to decrease more than twice as fast as the

362 average bag. Storage bag, fitting, and gasket material, as well as careful handling, are therefore important factors in

363 minimizing gas exchange. For example, silicone is permeable to CO_2, and thus could have been a path of gas exchange

364 into the tris for this experiment. As noted above, Nemzer and Dickson (2005) found an almost negligible change of

365 0.5 mpH yr^{-1} in bottled tris. Our bottled tris changed at -3.0 mpH yr^{-1} (n = 10 bottles measured over 161 days),

366 approximately half the rate of the tris stored in bags. While -3.0 mpH yr^{-1} is near the detection limit of our

367 measurements, it suggests that the bottling protocol used in this study was not as well controlled as that of Nemzer

368 and Dickson (2005). For example, the Dickson lab at Scripps Institution of Oceanography regularly uses an annealing

369 oven to combust all trace organic films that may persist on glass bottles, but in our study, bottles were not annealed.

370 Although bags cannot be annealed, future steps that may be worth consideration to reduce microbial respiration in

371 bags include addition of a biocide to the tris solution, acid cleaning the bags, and using ultraviolet light to remove

372 organics from the ultrapure water used to prepare tris. There are some disadvantages to these proposed steps. Addition

373 of a biocide may not be ideal for use in sensitive environments if the tris is discharged after use and would alter the

374 composition of the solution slightly. While rinsing or prolonged soaking of the bags with an acid may help to remove

375 organics, it is unclear if it would have negative effects on the integrity of the bags. Beyond removing organics on the

376 bag surfaces, care should be taken to avoid introducing organic contaminates into the tris during the solution

377 preparation and bag filling procedures to minimize future respiration.

378 Both bag type 1 and 2 experienced problems with structural integrity during this experiment. A single type 2

379 bag experienced delamination of exterior bag layers when stored submerged in seawater, causing the eventual tearing

380 and failure of the bag when handling. Bag type 2 was not used in test 3 due to this failure. It should be noted that in

381 other studies which successfully used bag type 2, the bag was submerged in seawater for less time than in this

382 experiment (Sayles and Eck, 2009; Aßmann et al., 2011; Wang et al., 2015). A single bag type 1 had the subtler

383 problem of small breaks in the aluminium foil bag layer, likely causing an increased pH rate of change. In non-

384 damaged bags, factors such as bag type/bottle, lab/tank storage, or tris batch did not have statistically significant (p-

385 value < 0.05) correlations with the pH change of tris (p-values 0.12, 0.11 and 0.09, respectively). The results of the

386 ANOVA support that tris can be held in bag type 1 or 2 and stored in a lab or tank and the pH will change similarly

387 regardless of storage method for up to 300 days. Additional bag types could be tested, such as bags made by Pollution

388 Measurement Corp. used by Lai et al. (2018) or Scholle DuraShield used by Takeshita et al. (2015).

389 These results suggest that when bags are carefully handled prior to and after filling, tris pH changes are small

390 over time. Specific recommendations for further work include: bags must be handled with care and enclosed in

391 protective containers to prevent damage, bags must be rinsed with tris prior to filling, and additional testing is merited

392 to determine sources of and methods to reduce contamination, such as acid washing.

Deleted: drift

Deleted: drift

Deleted: drifted

Deleted:

Deleted: the bag

Deleted:

Deleted: drift

Deleted: drift

Deleted: drift

4. Conclusions

This article describes our characterization of the stability of tris buffer in artificial seawater when stored in purportedly gas-impermeable bags. Several different tests, initiated over the course of a year and a half and lasting up to 300 days, exhibited an average decrease of 5.8 mpH yr^{-1}. In comparison, tris stored in standard borosilicate bottles was shown to have a decrease of 3.0 mpH yr^{-1}. For yearlong deployments, an expected pH change of -0.0058 is well below the weather quality threshold of 0.02 pH units. This low rate of change demonstrates the value of bagged tris for in situ validation of autonomous pH sensors (regardless of sensor operating principles), particularly in highly dynamic areas where repeatability of calibration based on discrete samples is challenging. Given the thorough characterization of tris over wide ranges of environmental variables, this contribution can aid in the traceability and intercomparability of pH sensor measurements. While valuable at the current stage of development (as demonstrated by, e.g., Lai et al. (2018) and Bresnahan et al. (2021)), further development would ideally result in a commercially available bag and filling procedure that can yield a rate of pH change less than the climate threshold of 0.003 per year. This will require further tests to identify the source of CO_2, gas exchange or microbial respiration, as well as steps to reduce or eliminate these sources.

Periodic measurement of bagged tris in situ would allow for detection of sensor drift. Most in situ pH sensors are deployed in the euphotic zone in coastal areas, typically resulting in expedited biofouling and sedimentation, and leading to sensor drift (Bresnahan et al., 2014) that could be identified and potentially corrected. Such periodic calibration/validation would aid in identifying sensor issues and allow for greater consistency and continuity between a timeseries and planned or vicarious crossovers where an automated calibration can be used to augment or replace pre- and post-deployment calibrations/validations.

Deleted: flexible and

Deleted: drift rates

Deleted: s

Deleted: –

Deleted: drift rate

Deleted: d

Deleted: of

Deleted: –

Deleted: drift

Deleted: still

Deleted: which allows for

Deleted: in coastal areas

434 **Appendix A**

435

436 **Table A1. Detailed information about the specific reagents used to make the tris solution. *Reagent chemicals that meet or**
437 **surpass specifications of the British Pharmacopeia (BP), European Pharmacopeia (EP), Food Chemicals Codex (FCC),**
438 **United States Pharmacopeia (USP).**

439

Chemical	Manufacture	Part Number	Lot Number	Batch	Assay	Grade
tris	Fisher Scientific	T395-1	170360	all	99.8%	Certified ACS
NaCl	Fisher Scientific	S641-212	127252	all	99.0 to 100.5%	*BP/EP/FCC/USP
Na_2SO_4	Fisher Scientific	S421-1	134837	all	99.8%	Certified ACS
KCl	Fisher Scientific	P217-500	174416	all	99.7%	Certified ACS
$MgCl_2$	Teknova	M0304	M030427E1401	all	1 M	Biotechnology
$CaCl_2$	Amresco	E506-500mL	0982C098	all	0.95-1.05 M	Biotechnology
HCl	Fisher Scientific	SA48-1	175004	1, 2, 3	0.999 N	Certified
HCl	Fisher Scientific	SA48-1	188768	4	1.003 N	Certified

440

441
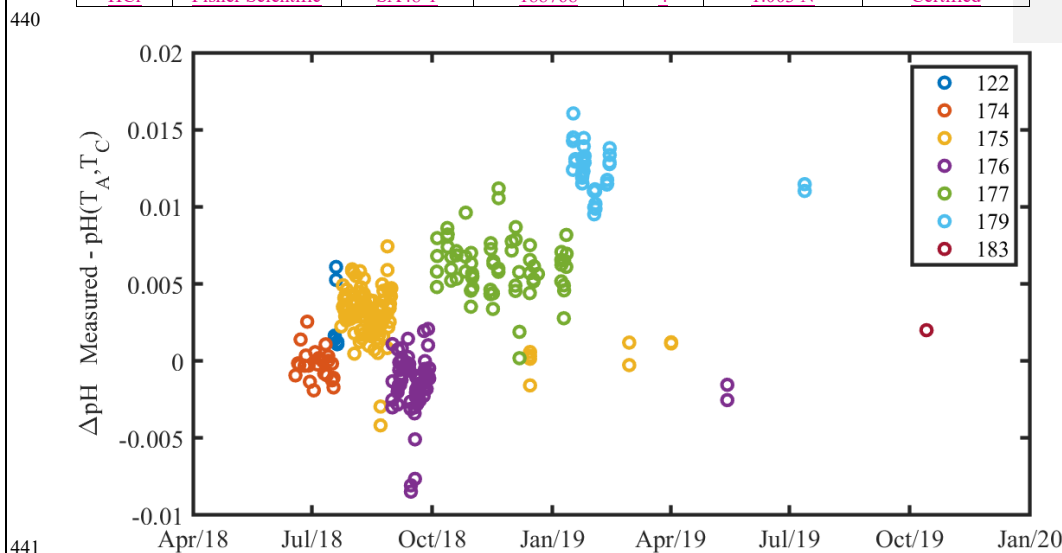
442 **Fig. A1: A timeseries of the residual between measured and calculated CRM pH throughout the experiment. Marker color**
443 **denotes CRM batch number. There is a clear variability between measured and calculated pH, which typical of CRM**
444 **batches (Andrew Dickson,** *pers. comm.***). There was no observable systematic drift in the pH system during the experiment.**
445 **The mean standard deviation of pH measurements within a CRM batch is 0.0016, which is comparable to the 0.0019**
446 **reported in Bockmon & Dickson (2015). The same 760 nm absorbance wavelength outlier removal procedure used for tris**
447 **measurements was applied to CRM measurements.**

448
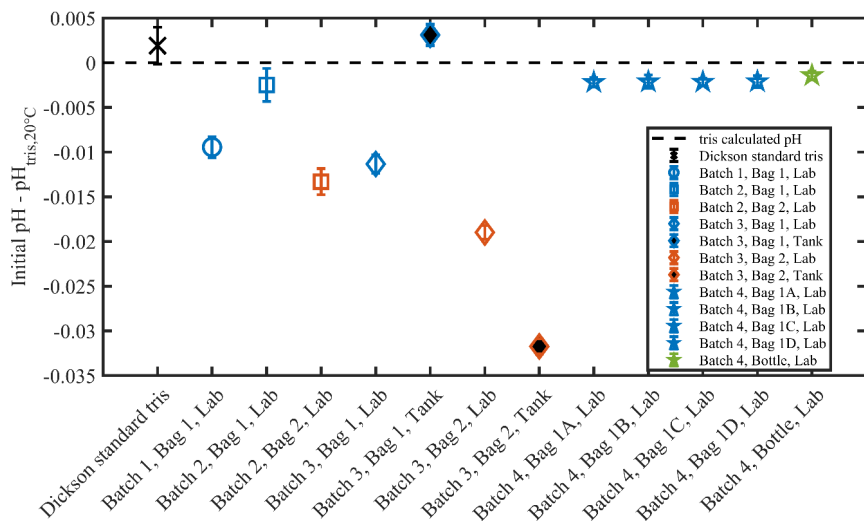
449

450 Fig. A2: The initial pH residual of each tris bag or bottle measured in this experiment. The initial pH is reported as a

451 residual from the calculated pH at 20 °C. The initial pH was measured directly for tris batch 4 and extrapolated for

452 tris batches 1-3. Additionally, 2 bottles of Dickson standard tris (show by the black "X") were measured on

453 12/10/2018. The zero black dashed line is the calculated pH of tris at 20 °C, based upon the measured reagent

454 concentrations (DelValls and Dickson, 1998).
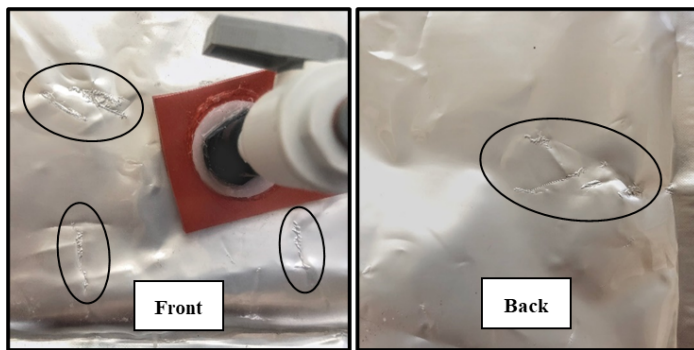
455

456 Fig. A3. The ovals indicate marks on the exterior of "Batch 2, Bag 1, Lab". These marks appear to be damage to the interior

457 metallic layer, possibly due to creasing of the bag. These marks were not present on any other bag used in this study.

458

459

Author contribution

WW performed formal analysis, visualization, and writing – original draft preparation. KS and TW contributed to investigation and writing – review & editing. PB, YT, and TM contributed to funding acquisition, conceptualization, formal analysis, and writing – review & editing.

Competing interests

The authors declare that they have no conflict of interest.

Data availability

pH and C_T data are available via the UC San Diego Library Digital Collections at https://doi.org/10.6075/J0QC022G (Wolfe et al., 2021).

Acknowledgements

We thank May-Linn Paulsen and Andrew Dickson's laboratory for sharing their tris expertise throughout this project. We thank the National Science Foundation Ocean Technology and Interdisciplinary Coordination (NSF-OTIC 1736905 and NSF-OTIC 1736864) and the David and Lucile Packard Foundation for supporting this work.

References

ACT: Protocols for the Performance Verification of In Situ pH Sensors, Alliance for Coastal Technologies, https://doi.org/10.25607/OBP-331, 2012.

Aßmann , S., Frank, C., and Kortzinger, A.: Spectrophotometric high-precision seawater pH determination for use in underway measuring systems, Ocean Sci., 7, 597-607, https://doi.org/10.5194/os-7-597-2011, 2011.

Bandstra, L., Hales, B., and Takahashi, T.: High-frequency measurements of total CO_2: Method development and first oceanographic observations, Mar. Chem., 100, 24-38, https://doi.org/10.1016/j.marchem.2005.10.009, 2006.

Bates, N., Astor, Y., Church, M., Currie, K., Dore, J., Gonzalez-Davila, M., Lorenzoni, L., Muller-Karger, F., Olafsson, J., and Santana-Casiano, J.: A Time-Series View of Changing Surface Ocean Chemistry Due to Ocean Uptake of Anthropogenic CO_2 and Ocean Acidification, J. Oceanogr., 27, 126-141, https://doi.org/10.5670/oceanog.2014.16, 2014.

Bittig, H. C., Steinhoff, T., Claustre, H., Fiedler, B., Williams, N. L., Sauzède, R., Körtzinger, A., and Gattuso, J.-P.: An Alternative to Static Climatologies: Robust Estimation of Open Ocean CO_2 Variables and Nutrient Concentrations From T, S, and O_2 Data Using Bayesian Neural Networks, Front. Mar. Sci., 5, https://doi.org/10.3389/fmars.2018.00328, 2018.

Bockmon, E. E., and Dickson, A. G.: An inter-laboratory comparison assessing the quality of seawater carbon dioxide measurements, Mar. Chem., 171, 36-43, https://doi.org/10.1016/j.marchem.2015.02.002, 2015.

Branch, T. A., DeJoseph, B. M., Ray, L. J., and Wagner, C. A.: Impacts of ocean acidification on marine seafood, Trends Ecol. Evol., 28, 178-186, https://doi.org/10.1016/j.tree.2012.10.001, 2013.

Bresnahan, P. J., Takeshita, Y., Wirth, T., Martz, T. R., Cyronak, T., Albright, R., Wolfe, K., Warren, J. K., and Mertz, K.: Autonomous in situ calibration of ion-sensitive field effect transistor pH sensors, Limnology and Oceanography: Methods, 19, 132-144, https://doi.org/10.1002/lom3.10410, 2021.

Bresnahan, P. J., Martz, T. R., Takeshita, Y., Johnson, K. S., and LaShomb, M.: Best practices for autonomous measurement of seawater pH with the Honeywell Durafet, Methods Oceanogr., 9, 44-60, https://doi.org/10.1016/j.mio.2014.08.003, 2014.

501 Bushinsky, S. M., Takeshita, Y., and Williams, N. L.: Observing changes in ocean carbonate chemistry: our
502   autonomous future, Curr. Clim, 5, 207-220, https://doi.org/10.1007/s40641-019-00129-8, 2019.
503 Byrne, R. H.: Measuring Ocean Acidification: New Technology for a New Era of Ocean Chemistry, Environ. Sci.
504   Technol., 48, 5352-5360, https://doi.org/10.1021/es405819p, 2014.
505 Carter, B., Radich, J., Doyle, H., and Dickson, A.: An automated system for spectrophotometric seawater pH
506   measurements, Limnol. Oceanogr. Methods, 11, 16-27, https://doi.org/10.4319/lom.2013.11.16, 2013.
507 Carter, B. R., Feely, R. A., Williams, N. L., Dickson, A. G., Fong, M. B., and Takeshita, Y.: Updated methods for
508   global locally interpolated estimation of alkalinity, pH, and nitrate, Limnol. Oceanogr. Methods, 16, 119-
509   131, https://doi.org/10.1002/lom3.10232, 2018.
510 Chavez, F., Pennington, J. T., Michisaki, R., Blum, M., Chavez, G., Friederich, J., Jones, B., Herlien, R., Kieft, B.,
511   Hobson, B., Ren, A., Ryan, J., Sevadjian, J., Wahl, C., Walz, K., Yamahara, K., Friederich, G., and Messié,
512   M.: Climate Variability and Change: Response of a Coastal Ocean Ecosystem, J. Oceanogr., 30, 128-145,
513   https://doi.org/10.5670/oceanog.2017.429, 2017.
514 Cooley, S. R., and Doney, S. C.: Anticipating ocean acidification's economic consequences for commercial fisheries,
515   Environ. Res. Lett., 4, 8, https://doi.org/10.1088/1748-9326/4/2/024007, 2009.
516 DeGrandpre, M. D., Spaulding, R. S., Newton, J. O., Jaqueth, E. J., Hamblock, S. E., Umansky, A. A., and Harris, K.
517   E.: Considerations for the measurement of spectrophotometric pH for ocean acidification and other studies,
518   Limnol. Oceanogr. Methods, 12, 830-839, https://doi.org/10.4319/lom.2014.12.830, 2014.
519 DelValls, T., and Dickson, A.: The pH of buffers based on 2-amino-2-hydroxymethyl-1,3-propanediol ('tris') in
520   synthetic sea water, Deep Sea Res. Part I, 45, 1541-1554, https://doi.org/10.1016/S0967-0637(98)00019-3,
521   1998.
522 Dickson, A. G.: pH buffers for sea-water media based on the total hydrogen-ion concentration scale, Deep Sea Res.
523   Part I, 40, 107-118, https://doi.org/10.1016/0967-0637(93)90055-8, 1993.
524 Dickson, A. G.: Reference materials for oceanic CO_2 measurements, J. Oceanogr., 14, 21-22, 2001.
525 Dickson, A. G., Sabine, C. L., and Christian, J. R.: Guide to Best Practices for Ocean CO_2 Measurements, PICES
526   Special Publication 3, North Pacific Marine Science Organization, Sidney, British Columbia, 191 pp., 2007.
527 Doney, S. C., Fabry, V. J., Feely, R. A., and Kleypas, J. A.: Ocean acidification: the other CO_2 problem, Annu. Rev.
528   Mar. Science, 1, 169-192, https://doi.org/10.1146/annurev.marine.010908.163834, 2009.
529 Doney, S. C., Busch, D. S., Cooley, S. R., and Kroeker, K. J.: The impacts of ocean acidification on marine ecosystems
530   and reliant human communities, Annu. Rev. Environ. Resour., 45, https://doi.org/10.1146/annurev-environ-
531   012320-083019, 2020.
532 Friederich, G., Walz, P., Burczynski, M., and Chavez, F.: Inorganic carbon in the central California upwelling system
533   during the 1997–1999 El Niño–La Niña event, Prog. Oceanogr., 54, 185-203, https://doi.org/10.1016/S0079-
534   6611(02)00049-6, 2002.
535 Hales, B., Takahashi, T., and Bandstra, L.: Atmospheric CO_2 uptake by a coastal upwelling system, Global
536   Biogeochem. Cycles, 19, https://doi.org/10.1029/2004gb002295, 2005.
537 Johnson, K. S., Jannasch, H. W., Coletti, L. J., Elrod, V. A., Martz, T. R., Takeshita, Y., Carlson, R. J., and Connery,
538   J. G.: Deep-Sea DuraFET: A Pressure Tolerant pH Sensor Designed for Global Sensor Networks, Anal.
539   Chem., 88, 3249-3256, https://doi.org/10.1021/acs.analchem.5b04653, 2016.
540 Johnson, K. S., Plant, J. N., Coletti, L. J., Jannasch, H. W., Sakamoto, C. M., Riser, S. C., Swift, D. D., Williams, N.
541   L., Boss, E., Haëntjens, N., Talley, L. D., and Sarmiento, J. L.: Biogeochemical sensor performance in the
542   SOCCOM   profiling   float   array,   J.   Geophys.   Res.:   Oceans,   122,   6416-6436,
543   https://doi.org/10.1002/2017jc012838, 2017.
544 Karl, D. M.: Oceanic ecosystem time-series programs: Ten lessons learned, J. Oceanogr., 23, 104-125,
545   https://doi.org/10.5670/oceanog.2010.27, 2010.
546 Lai, C.-Z., DeGrandpre, M. D., and Darlington, R. C.: Autonomous Optofluidic Chemical Analyzers for Marine
547   Applications: Insights from the Submersible Autonomous Moored Instruments (SAMI) for pH and pCO₂,
548   Front. Mar. Sci., 4, https://doi.org/10.3389/fmars.2017.00438, 2018.
549 Liu, X. W., Patsavas, M. C., and Byrne, R. H.: Purification and Characterization of meta-Cresol Purple for
550   Spectrophotometric   Seawater   pH   Measurements,   Environ.   Sci.   Technol.,   45,   4862-4868,
551   https://doi.org/10.1021/es200665d, 2011.
552 Martz, T. R., Daly, K. L., Byrne, R. H., Stillman, J. H., and Turk, D.: Technology for ocean acidification research
553   needs and availability, J. Oceanogr., 28, 40-47, https://doi.org/10.5670/oceanog.2015.30, 2015.
554 McLaughlin, K., Dickson, A., Weisberg, S. B., Coale, K., Elrod, V., Hunter, C., Johnson, K. S., Kram, S., Kudela, R.,
555   Martz, T., Negrey, K., Passow, U., Shaughnessy, F., Smith, J. E., Tadesse, D., Washburn, L., and Weis, K.

556   R.: An evaluation of ISFET sensors for coastal pH monitoring applications, Reg. Stud. Mar. Sci., 12, 11-18,
557   https://doi.org/10.1016/j.rsma.2017.02.008, 2017.
558 Müller, J., Bastkowski, F., Sander, B., Seitz, S., Turner, D., Dickson, A., and Rehder, G.: Metrology for pH
559   Measurements in Brackish Waters-Part 1: Extending Electrochemical pH(T) Measurements of TRIS Buffers
560   to Salinities 5-20, Front. Mar. Sci., 5, https://doi.org/10.3389/fmars.2018.00176, 2018.
561 Müller, J. D., and Rehder, G.: Metrology of pH Measurements in Brackish Waters—Part 2: Experimental
562   Characterization of Purified meta-Cresol Purple for Spectrophotometric pHT Measurements, Front. Mar.
563   Sci., 5, 177, https://doi.org/10.3389/fmars.2018.00177, 2018.
564 Nemzer, B., and Dickson, A.: The stability and reproducibility of Tris buffers in synthetic seawater, Mar. Chem., 96,
565   237-242, https://doi.org/10.1016/j.marchem.2005.01.004, 2005.
566
567 Newton, J., Feely, R., Jewett, E., Williamson, P., and Mathis, J.: Global Ocean Acidification Observing Network:
568   Requirements and Governance Plan. Second Edition, 2015.
569 O'Sullivan, D. W., and Millero, F. J.: Continual measurement of the total inorganic carbon in surface seawater, Mar.
570   Chem., 60, 75-83, https://doi.org/10.1016/s0304-4203(97)00079-0, 1998.
571 Okazaki, R. R., Sutton, A. J., Feely, R. A., Dickson, A. G., Alin, S. R., Sabine, C. L., Bunje, P. M. E., and Virmani,
572   J. I.: Evaluation of marine pH sensors under controlled and natural conditions for the Wendy Schmidt Ocean
573   Health XPRIZE, Limnol. Oceanogr. Methods, 15, 586-600, https://doi.org/10.1002/lom3.10189, 2017.
574 Paulsen, M. L., and Dickson, A. G.: Preparation of 2-amino-2-hydroxymethyl-1, 3-propanediol (TRIS) pHT buffers
575   in synthetic seawater, Limnol. Oceanogr. Methods, 18, 504-515, https://doi.org/10.1002/lom3.10383, 2020.
576 Papadimitriou, S., Loucaides, S., Rérolle, V., Achterberg, E. P., Dickson, A. G., Mowlem, M., and Kennedy, H.: The
577   measurement of pH in saline and hypersaline media at sub-zero temperatures: Characterization of Tris
578   buffers, Mar. Chem., 184, 11–20, https://doi.org/10.1016/j.marchem.2016.06.002, 2016.
579 Pierrot, D., Neill, C., Sullivan, K., Castle, R., Wanninkhof, R., Lüger, H., Johannessen, T., Olsen, A., Feely, R. A.,
580   and Cosca, C. E.: Recommendations for autonomous underway pCO_2 measuring systems and data-reduction
581   routines, Deep Sea Res. Part II, 56, 512-522, https://doi.org/10.1016/j.dsr2.2008.12.005, 2009.
582 Rodriguez, C., Huang, F., and Millero, F. J.: The partial molal volume and compressibility of Tris and Tris–HCl in
583   water and 0.725 m NaCl as a function of temperature, Deep Sea Res. Part I, 104, 41-51,
584   https://doi.org/10.1016/j.dsr.2015.06.008, 2015.
585 Sabine, C., Sutton, A., McCabe, K., Lawrence-Slavas, N., Alin, S., Feely, R., Jenkins, R., Maenner, S., Meinig, C.,
586   and Thomas, J.: Evaluation of a new carbon dioxide system for autonomous surface vehicles, J. Atmos.
587   Oceanic Technol., 37, 1305-1317, https://doi.org/10.1175/JTECH-D-20-0010.1, 2020.
588 Sayles, F. L., and Eck, C.: An autonomous instrument for time series analysis of TCO_2 from oceanographic moorings,
589   Deep Sea Res. Part I, 56, 1590-1603, https://doi.org/10.1016/j.dsr.2009.04.006, 2009.
590 Seidel, M. P., DeGrandpre, M. D., and Dickson, A. G.: A sensor for in situ indicator-based measurements of seawater
591   pH, Mar. Chem., 109, 18-28, https://doi.org/10.1016/j.marchem.2007.11.013, 2008.
592 Sloyan, B. M., Wanninkhof, R., Kramp, M., Johnson, G. C., Talley, L. D., Tanhua, T., McDonagh, E., Cusack, C.,
593   O'Rourke, E., McGovern, E., Katsumata, K., Diggs, S., Hummon, J., Ishii, M., Azetsu-Scott, K., Boss, E.,
594   Ansorge, I., Perez, F. F., Mercier, H., Williams, M. J. M., Anderson, L., Lee, J. H., Murata, A., Kouketsu, S.,
595   Jeansson, E., Hoppema, M., and Campos, E.: The Global Ocean Ship-Based Hydrographic Investigations
596   Program (GO-SHIP): A Platform for Integrated Multidisciplinary Ocean Sci., Front. Mar. Sci., 6,
597   https://doi.org/10.3389/fmars.2019.00445, 2019.
598 Spaulding, R. S., DeGrandpre, M. D., Beck, J. C., Hart, R. D., Peterson, B., De Carlo, E. H., Drupp, P. S., and Hammar,
599   T. R.: Autonomous in Situ Measurements of Seawater Alkalinity, Environ. Sci. Technol., 48, 9573-9581,
600   https://doi.org/10.1021/es501615x, 2014.
601 Sutton, A. J., Feely, R. A., Maenner-Jones, S., Musielwicz, S., Osborne, J., Dietrich, C., Monacci, N., Cross, J., Bott,
602   R., and Kozyr, A.: Autonomous seawater pCO_2 and pH time series from 40 surface buoys and the emergence
603   of anthropogenic trends, Earth Syst. Sci. Data, 421, https://doi.org/10.5194/essd-11-421-2019, 2019.
604 Takeshita, Y., Frieder, C. A., Martz, T. R., Ballard, J. R., Feely, R. A., Kram, S., Nam, S., Navarro, M. O., Price, N.
605   N., and Smith, J. E.: Including high-frequency variability in coastal ocean acidification projections,
606   Biogeosciences, 12, 5853-5870, https://doi.org/10.5194/bg-12-5853-2015, 2015.
607 Takeshita, Y., McGillis, W., Briggs, E. M., Carter, A. L., Donham, E. M., Martz, T. R., Price, N. N., and Smith, J. E.:
608   Assessment of net community production and calcification of a coral reef using a boundary layer approach,
609   J. Geophys. Res.: Oceans, 121, 5655-5671, https://doi.org/10.1002/2016JC011886, 2016.
610 Takeshita, Y., Martz, T. R., Coletti, L. J., Dickson, A. G., Jannasch, H. W., and Johnson, K. S.: The effects of pressure
611   on pH of Tris buffer in synthetic seawater, Mar. Chem., 188, 1-5, 10.1016/j.marchem.2016.11.002, 2017.

616 Takeshita, Y., Johnson, K. S., Martz, T. R., Plant, J. N., and Sarmiento, J. L.: Assessment of Autonomous pH
617   Measurements for Determining Surface Seawater Partial Pressure of CO_2, J. Geophys. Res.: Oceans, 123,
618   4003-4013, https://doi.org/10.1029/2017jc013387, 2018.
619 Takeshita, Y., et al.: Consistency and stability of purified meta-cresol purple for spectrophotometric pH measurements
620   in seawater, Mar. Chem., in review.
621 Tilbrook, B., Jewett, E. B., DeGrandpre, M. D., Hernandez-Ayon, J. M., Feely, R. A., Gledhill, D. K., Hansson, L.,
622   Isensee, K., Kurz, M. L., Newton, J. A., Siedlecki, S. A., Chai, F., Dupont, S., Graco, M., Calvo, E., Greeley,
623   D., Kapsenberg, L., Lebrec, M., Pelejero, C., Schoo, K. L., and Telszewski, M.: An Enhanced Ocean
624   Acidification Observing Network: From People to Technology to Data Synthesis and Information Exchange,
625   Front. Mar. Sci., 6, 21, https://doi.org/10.3389/fmars.2019.00337, 2019.
626 Wang, Z. A., Sonnichsen, F. N., Bradley, A. M., Hoering, K. A., Lanagan, T. M., Chu, S. N., Hammar, T. R., and
627   Camilli, R.: In Situ Sensor Technology for Simultaneous Spectrophotometric Measurements of Seawater
628   Total Dissolved Inorganic Carbon and pH, Environ. Sci. Technol., 49, 4441-4449,
629   https://doi.org/10.1021/es504893n, 2015.
630 Wang, Z. A., Moustahfid, H., Mueller, A. V., Michel, A. P. M., Mowlem, M., Glazer, B. T., Mooney, T. A., Michaels,
631   W., McQuillan, J. S., Robidart, J. C., Churchill, J., Sourisseau, M., Daniel, A., Schaap, A., Monk, S.,
632   Friedman, K., and Brehmer, P.: Advancing Observation of Ocean Biogeochemistry, Biology, and
633   Ecosystems With Cost-Effective in situ Sensing Technologies, Front. Mar. Sci., 6, 22,
634   https://doi.org/10.3389/fmars.2019.00519, 2019.
635 Williams, N. L., Juranek, L. W., Johnson, K. S., Feely, R. A., Riser, S. C., Talley, L. D., Russell, J. L., Sarmiento, J.
636   L., and Wanninkhof, R.: Empirical algorithms to estimate water column pH in the Southern Ocean, Geophys.
637   Res. Lett., 43, 3415-3422, https://doi.org/10.1002/2016gl068539, 2016.
638 Wolfe, W. H., Shipley, K. M., Bresnahan, P. J., Takeshita, Y., Wirth, T., Martz, T. R.: Data from: Technical note:
639   stability of tris pH buffer in artificial seawater stored in bags. UC San Diego Library Digital
640   Collections. https://doi.org/10.6075/J0QC022G, 2021.